DOI: 10.1021/cg1011605

CRYSTAL GROWTH & DESIGN Article

2010, Vol. 10
5302–5306

Hirshfeld Surface Analysis of Substituted Phenols

Adam D. Martin, Karel J. Hartlieb, Alexandre N. Sobolev, and Colin L. Raston*

Centre for Strategic Nano-Fabrication, School of Biomedical, Biomolecular and Chemical Sciences, University of Western Australia, 35 Stirling Highway, Crawley, WA 6009, Australia

Received September 1, 2010; Revised Manuscript Received October 15, 2010

ABSTRACT: The effect of *para*-substituents on the crystal packing of phenols has been investigated, for systems bearing nonpolar groups (*tert*-butyl and benzyl, compounds **1** and **2**, respectively) and for methylene linked bis-phenol bearing polar nitro groups (compound **3**). Remarkable for **1** and **2**, the asymmetric unit has six molecules, which form infinite helical hydrogen bonded arrays in the extended structures, whereas compound **3** bearing nitro groups coplanar with the phenol rings forms almost columnar arrays. Hirshfeld surface analysis is used to show that despite packing in a nearly identical manner, **1** and **2** are distinctly different in their interactions, and these structures are compared to compound **3**, where the solid-state interactions are dominated by the nitro moieties.

Introduction

Phenolic compounds feature in a wide variety of processes, such as in self-assembly,[1] the purification of nucleic acids,[2] and as key reagents in chemical synthesis.[3] *para*-*tert*-Butylphenol is well-known as the adhesive resin in Bakelite in combination with formaldehyde[4] and as the main phenol used for preparing calix[*n*]arenes.[5] Variations in solvent, base, and stoichiometry allows access to *para*-*tert*-butylcalix[*n*]arenes where the number of phenol units [*n*] can vary from 4 to 20.[6] *para*-Benzylphenol features in the base catalyzed condensation of calix[*n*]arenes, affording a mixture of macrocycles, $n = 5-8$,[7] or predominantly $n = 4$,[8] which forms solid-state inclusion compounds with icosahedral *ortho*-carborane and C_{60}.[9] *para*-Nitrophenol is a well-known intermediate in the synthesis of paracetamol,[10] and 2,2-methylene bis(4-nitrophenol) has been used in the preparation of nitrated "double calixarenes"[11] and nitrated macrocyclic polyethers.[12] Substitution at the *meta*- and *ortho*-positions of phenol also plays a significant role in phenol-based chemistry, but the focus of the present work is on the *para*-substitution because of the nexus with calixarenes.

Hirshfeld surface analysis is rapidly gaining prominence as a powerful technique in understanding the nature of intermolecular interactions within a crystal structure using a fingerprint plot. This allows easy identification of characteristic interactions throughout the structures,[13] or as a surface around the molecule.[14] A d_{norm} surface allows for easy comparison of intermolecular contacts relative to van der Waals radii by way of a simple red−white−blue color scheme. Recently, this system has been applied to large macromolecular structures such as *para*-alkylated calix[4]arenes,[15] and *para*-substituted calix[5]arenes as C_{70} complexes,[16] in addition to smaller molecules such as 2-chloro-4-nitrbenzoic acid.[17]

Results and Discussion

para-*tert*-Butylphenol, **1** (Figure 1), was crystallized by evaporation of a hot acetonitrile solution, *para*-benzylphenol, **2**, was crystallized by slow evaporation from a benzene solution, and crystals of 2,2-methylene bis(4-nitrophenol), **3**, were formed during the solventless synthesis of the compound by grinding *para*-nitrophenol with paraformaldehyde.

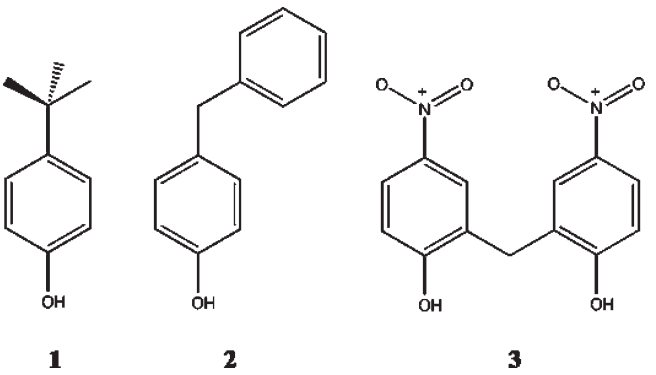

Figure 1. Molecular structures of the compounds investigated in this study.

Compound **1** crystallizes in the triclinic space group $P\bar{1}$, with six molecules in the asymmetric unit. The large complex asymmetric unit for such a small molecule in part explains why this important and abundant compound has not been previously structurally authenticated. For two crystallographically independent molecules, the *tert*-butyl group is disordered over two positions, each with a modeled occupancy of 0.50. Packing results in a continuous network of hydrogen bonding (OH···O 2.649(2)−2.691(2) Å) involving the phenolic hydroxyl groups, forming a helical array along the *a* axis (Figure 2a). The *tert*-butyl groups are mostly oriented toward the phenyl ring of a neighboring molecule, with some interactions, as evidenced in the packing diagram.

The Hirshfeld surface analysis shows a similar proportion of O···H contacts for each of the six molecules, ranging from 5.6 to 6.0%. In all cases, the O···H interactions are represented by a spike in the bottom left (donor) area of the fingerprint plot (Figure 2b), which represents a phenolic oxygen interacting with a neighboring phenolic hydrogen, forming the helical network of hydrogen bonds. The H···O interactions are represented by a spike in the bottom right region of the fingerprint plot, and the proportion of H···O interactions has a larger variance than its O···H counterparts, ranging from 3.8 to 6.2%. Only one

*To whom correspondence should be addressed. Fax: +618 6488 1005. E-mail: colin.raston@uwa.edu.au.

 Published on Web 11/08/2010

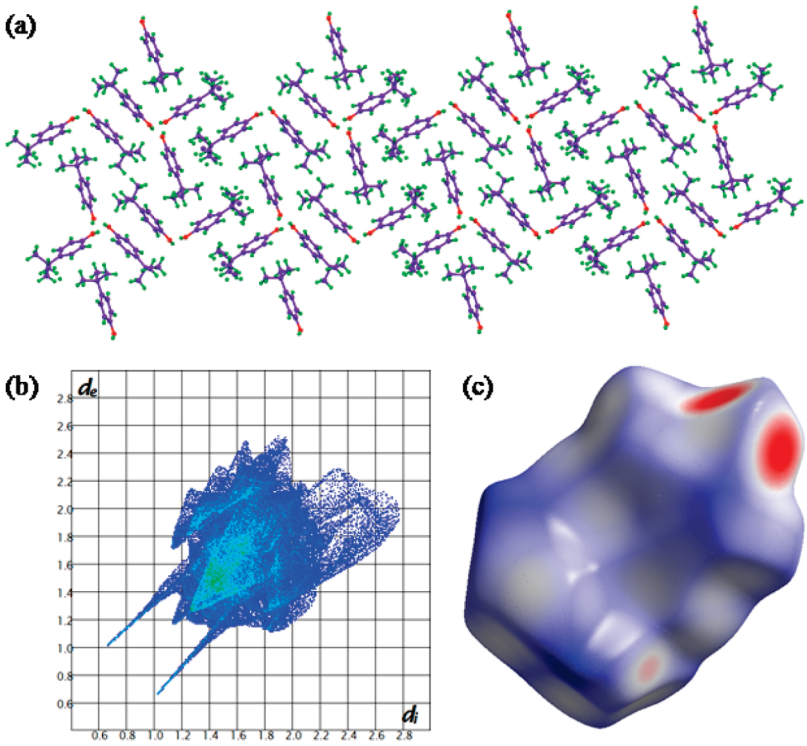

Figure 2. (a) Packing diagram, (b) Hirshfeld surface fingerprint plot, and (c) and the d_{norm} surface of *p*-*tert*-butylphenol, **1**.

molecule displays a higher proportion of H···O than O···H interactions, and this is due to two of its *tert*-butyl protons interacting with a nearby phenolic oxygen. These oxygen-based interactions represent the closest contacts in the structure and can be viewed as a pair of large red spots on the d_{norm} surface (Figure 2c).

The "wings" seen in the plot belong to signature CH···π interactions, with the "wing" in the lower right of the fingerprint plot representing CH···π acceptor (or C···H) interactions. The proportion of C···H interactions vary from 10.2 to 14.4% and are mainly due to neighboring *tert*-butyl groups pointing toward the aromatic ring of the phenol moiety. H···C interactions vary from 6.3 to 8.5% and are mainly due to the *tert*-butyl groups, with one molecule displaying a larger, more diffuse H···C area in its fingerprint plot, and this relates to the methyl group being oriented into a void in the crystal structure and is associated with a myriad of long contacts. Interestingly, one of the molecules in the structure does not display any "wings", and thus, despite possessing C···H and H···C interactions, no CH···π acceptor or donor interactions are present.

The majority of contacts, however, are due to H···H interactions, with these interactions making up 59.6 to 76.0% of the Hirshfeld surface of these molecules. These contacts are mainly due to the *tert*-butyl groups, although one of the molecules has a short contact where an *ortho*-hydrogen interacts with a proton from a neighboring *tert*-butyl group.

p-Benzylphenol, **2**, crystallizes in the orthorhombic space group $Pna2_1$, with the asymmetric unit remarkably also consisting of six molecules ($Z = 24$). No solvents or disorder are present in the structure. It packs in a manner very similar to that of compound **1**, with a continuous network of hydrogen bonding (OH···O 2.641(5)−2.670(5) Å) in the form of a helical array down the *b* axis (Figure 3a). The replacement of a *tert*-butyl group with a benzyl group possessing an aromatic ring results in a larger proportion of CH···π interactions. There is a pseudoinversion center, at 1/8, 1/2, 1/2, which is common for molecular structures crystallizing in the space group $Pna2_1$ when $Z > 4$.[18]

The Hirshfeld surface analysis shows that the proportion of O···H interactions is similar for each of the six crystallographically independent molecules, ranging from 4.9 to 5.9%, while the proportion of H···O interactions range from to 2..7 to 5.1%. The nature of the interactions are very similar to those seen in compound **1**, where the phenolic hydrogen interacts with a neighboring phenolic oxygen, with hydrogen interacting with another neighboring phenolic oxygen and so forth, building a helical network of hydrogen bonds throughout the structure. These short oxygen-based contacts are identified once again on the d_{norm} Hirshfeld surface of the molecules as large red spots (Figure 3b).

The C···H and H···C regions of the fingerprint plots for this structure are notable in that four of the six unique molecules are involved only in CH···π acceptor or donor interactions, not both, resulting in the appearance of only one "wing" in the fingerprint plot. The proportion of C···H interactions range from 17.8 to 20.7%, which is much larger than that for compound **1**. This can be directly attributed to the nature of the *para*-substituent, with the benzyl group resulting in more C···H interactions than the *tert*-butyl group in compound **1**. The primary type of CH···π interactions arise from either a *meta* hydrogen from a neighboring benzyl group pointing toward the phenyl aromatic ring or a *meta* hydrogen from a neighboring phenyl group pointing toward a neighboring benzyl aromatic ring. The proportion of H···C interactions vary from 11.5 to 18.6%, and the nature of the interactions are similar to those described for C···H interactions. A stunning feature of the Hirshfeld surface analysis is the complementarity of the CH···π donor and acceptor regions for fingerprint plots of two separate molecules (Figure 3c and d), where one molecule displays a strong CH···π donor "wing", and a neighboring molecule displays a strong CH···π acceptor "wing".

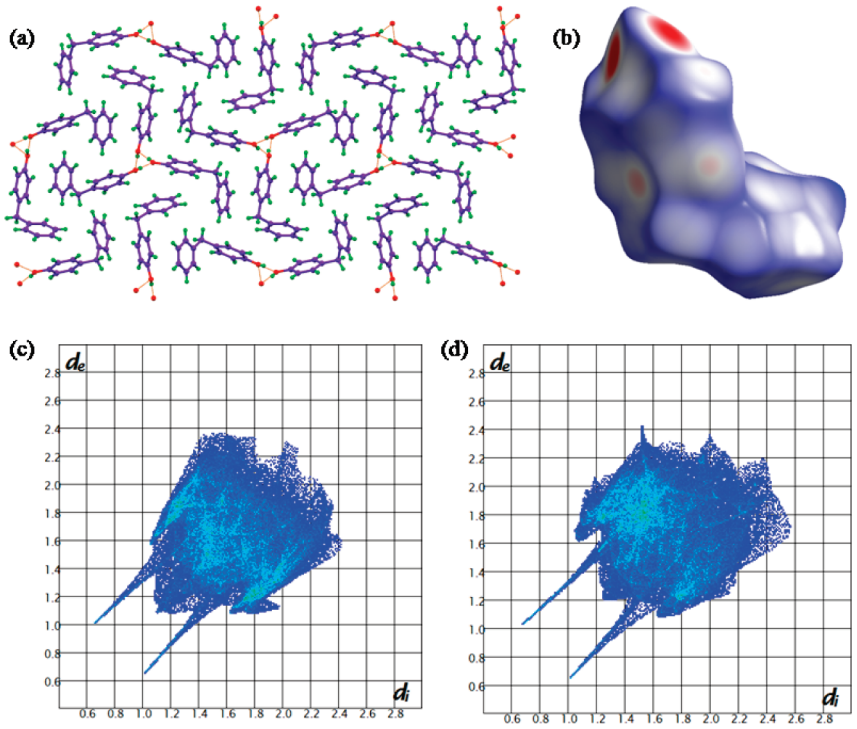

Figure 3. (a) Packing diagram displaying the network of hydrogen bonding, (b) d_{norm} Hirshfeld surface, and (c and d) complementarity of the CH···π donor "wing" of one molecule (c, bottom right) with the CH···π acceptor "wing" of another molecule (d, top left) in compound **2**.

The majority of the other contacts are H···H interactions, with the proportion of these varying from 50.9 to 59.2%, which is notably less than that for compound **1**, and again, it relates to the presence of the benzyl substituent. Short contacts arise where a *meta*-hydrogen interacts closely with a neighboring methylene proton and where a *meta*-hydrogen from a phenyl interacts with a *meta*-hydrogen from a neighboring benzyl moiety.

Compound **3** crystallizes in the triclinic space group $P\bar{1}$, with two molecules of 2,2′-methylene bis(4-nitrophenol) in the asymmetric unit ($Z = 4$). No solvents or disorder are observed in the structure. Viewing the packing of the structure down the *b* axis shows an almost columnar arrangement of molecules, with the phenyl rings being angled at 114° relative to each other, meaning that one phenyl group of the molecule is oriented down the *b* axis, while the other phenyl group is oriented almost orthogonal to this axis (Figure 4a). This combined with the nitro groups being oriented opposite to each other in the structure means that each nitro group interacts with a hydroxyl from an orthogonal phenyl ring. Thus, unlike in compounds **1** or **2**, there is no helical arrangement of hydrogen bonding (OH···O 2.781(5)−2.933(5) Å), instead the hydrogen bonding in the structure is limited to these "columns". The methylene linker between the phenol moieties plays a negligible electronic role in the packing of this structure, the interactions between the nitro groups dominating the orientation of the phenol rings and the overall packing/cohesion of the structure.

Oxygen-based interactions play a much larger part in the structure of compound **3** than in the structures of compounds **1** and **2** due to the presence of the nitro substituent. The proportion of O···H interactions is 22.3 and 22.4% for the two molecules, and the proportion of H···O interactions is 19.1 and 20.3%. One of the prominent short contacts is due to an oxygen from a nitro group interacting with a hydrogen from a neighboring phenolic group. Another short contact arises where the other oxygen from the same nitro group interacts with a *meta*-hydrogen from a neighboring phenyl unit. The most interesting interaction, however, is from the other nitro group on the molecule, where both of the oxygen atoms are involved in an interaction with a neighboring phenolic hydrogen, which is oriented between the nitro groups. This is responsible for a distinctive red double spot on the d_{norm} surface (Figure 4c).

The proportion of C···H interactions are similar to those seen in compound **1**, with these interactions comprising 9.7 and 10.0% of the Hirshfeld surface for each molecule. Two instances of CH···π interactions are responsible for the "wings" which are evident in the fingerprint plot, one where a neighboring *meta*-hydrogen is pointing toward the middle of one aromatic ring, seen on the d_{norm} surface as a hexagonal-shaped red spot in Figure 4d, and the other where a neighboring methylene proton is oriented toward the center of the other aromatic ring of the molecule. The H···C interactions are responsible for 7.4 and 8.9% of the Hirshfeld surface of the molecules and are the reverse of the C···H interactions, which can be seen by the symmetrical nature of this area in the fingerprint plot.

It is noteworthy that H···H interactions only represent a small part of the Hirshfeld surface, unlike for compounds **1** and **2**. This is to be expected due to the nitro substituents, and H···H interactions comprise only 18.2% of the Hirshfeld surface for both molecules. Short H···H contacts result from two neighboring methylene hydrogens interacting with each other, or two neighboring *meta*-hydrogen atoms interacting with each other. Nevertheless, these two exceptions aside, the H···H interactions are mainly associated with long contacts.

O···O interactions make up 5.9 and 6.2% of the Hirshfeld surface of the molecules in the structure, mainly for oxygen atoms from the nitro group interacting directly with neighboring phenolic oxygens (involving hydrogen bonding). Another interesting feature is the occurrence of C···C interactions,

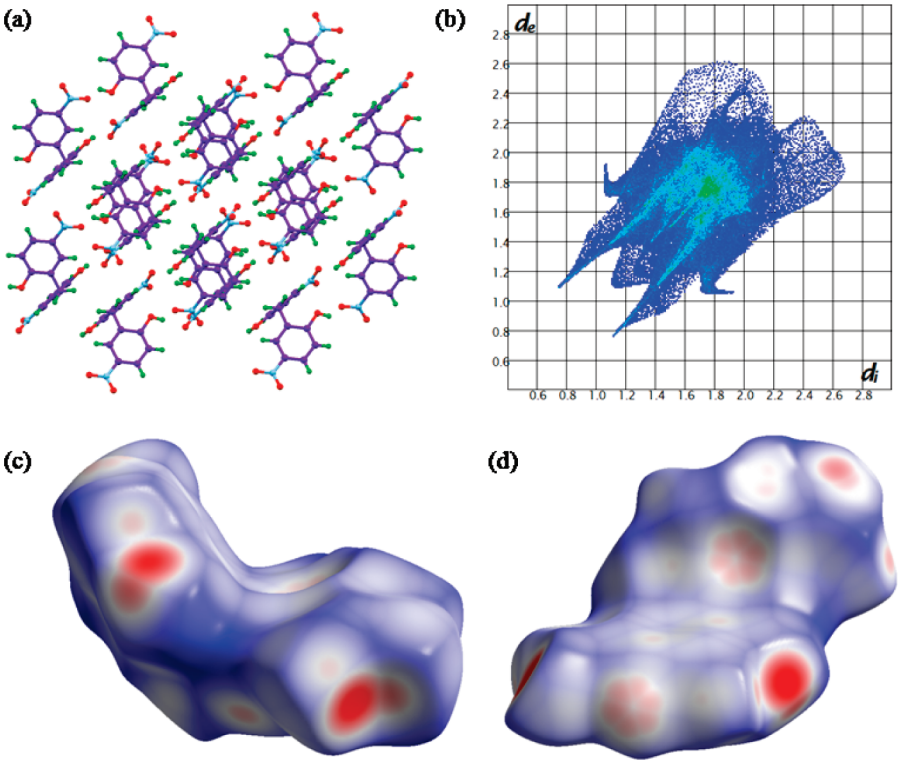

Figure 4. (a) Packing diagram, (b) fingerprint plot, (c) d_{norm} surface displaying the "double spot" due to an O···H interaction, and (d) d_{norm} surface displaying a CH···π donor and acceptor contacts for compound **3**.

which are responsible for 5.4 and 5.7% of the Hirshfeld surface, revealing the presence of $\pi\cdots\pi$ stacking within the structure. In each molecule, there are two instances of C···C interactions for each phenyl ring, one due to a CH···π interaction and one due to a $\pi\cdots\pi$ interaction.

We have shown that the *para*-phenol substituents play a significant role in the solid state behavior of the three phenol compounds, and for **1** and **2**, this is despite their very similar packing motifs. Compounds **1** and **2** form infinite O···HO hydrogen bonded helical arrays, in contrast to the typical cyclic hydrogen bonded arrays when the same molecules are condensed with formaldehyde in forming the ubiquitous calixarene macrocycles. Hirshfeld surface analyses revealed that (i) a *tert*-butyl moiety results in dominant H···H interactions, (ii) a benzyl moiety results in dominant carbon-based interactions, and (iii) a nitro moiety results in the prevalence of oxygen-based interactions, noting that such information is not readily apparent from conventional analysis of the crystal packing diagrams alone. All three compounds investigated in this study are important precursors for calixarenes and other supramolecular architectures, and understanding the behavior of these monomeric units themselves provides valuable insight into the solid-state behavior of larger molecules which covalently incorporate these compounds.

Experimental Section

All compounds used in this study were purchased from commercial sources and used without further purification.

Crystallography. For compound **1**, the X-ray diffracted intensities were measured from a single crystal, 0.43 × 0.17 × 0.13 mm^3, at about 100 K on an Oxford Diffraction Xcalibur CCD diffractometer using monochromatized Mo-K_α (λ = 0.71073 Å.)

For compounds **2** and **3**, the X-ray diffracted intensities were measured from a colorless single crystal, 0.33 × 0.09 × 0.05 mm^3, at about 100 K on an Oxford Diffraction Gemini-R Ultra CCD diffractometer using monochromatized Cu-K_α (λ = 1.54178 Å).

Data were corrected for Lorentz and polarization effects and absorption correction applied using multiple symmetry equivalent reflections. The structure was solved by the direct method and refined on F^2 using the SHELX-97 crystallographic package[19] and X-Seed interface.[20] A full matrix least-squares refinement procedure was used, minimizing $w(F_o^2 - F_c^2)$, with $w = [\sigma^2(F_o^2) + (AP)^2 + BP]^{-1}$, where $P = (F_o^2 + 2F_c^2)/3$. Agreement factors ($R = \Sigma||F_o| - |F_c||/\Sigma|F_o|$, $wR2 = \{\Sigma[w(F_o^2 - F_c^2)^2]/\Sigma[w(F_o^2)^2]\}^{1/2}$, and GOF = $\{\Sigma[w(F_o^2 - F_c^2)^2]/(n-p)\}^{1/2}$) are cited, where n is the number of reflections and p the total number of parameters refined. Non-hydrogen atoms of nondisordered fragments were refined anisotropically using all reflections. The positions of hydrogen atoms partly were localized from the difference Fourier map and partly calculated from geometrical consideration, and their atomic parameters were constrained to the bonded atoms during the refinement. Hirshfeld surface analysis was undertaken using CrystalExplorer 2.1.[21] CCDC deposition numbers are 787583−787585.

Crystal/Refinement Details for 1. $C_{10}H_{14}O$, M = 150.21, colorless wedge 0.43 × 0.17 × 0.13 mm, $F(000)$ = 984 e, triclinic, $P\bar{1}$ (No. 2), Z = 12, T = 100(2) K, a = 6.2213(2), b = 11.9145(4), c = 37.398(1) Å, α = 98.779(3), β = 93.944(2), γ = 93.235(2)°, V = 2726.81(15) Å^3; D_c = 1.098 g cm^{-3}; $\sin\theta/\lambda_{max}$ = 0.5946; N(unique) = 9614 (merged from 43172, R_{int} = 0.0376, R_{sig} = 0.0561), N_o ($I > 2\sigma(I)$) = 5677; R = 0.0559, $wR2$ = 0.1458 (A,B = 0.09, 0.0), GOF = 1.001; $|\Delta\rho_{max}|$ = 0.49(4) e Å^{-3}.

Crystal/Refinement Details for 2. $C_{13}H_{12}O$, M = 184.23, colorless needle 0.33 × 0.09 × 0.05 mm, $F(000)$ = 2352 e, orthorhombic, $Pna2_1$ (No. 33), Z = 24, T = 100(2) K, a = 42.858(3), b = 6.0745(3), c = 23.1726(11) Å, V = 6032.8(6), Å^3; D_c = 1.217 g cm^{-3}; μ_{Cu} = 0.589 mm^{-1}; $\sin\theta/\lambda_{max}$ = 0.5877; N(unique) = 5246 (merged from 57834, R_{int} = 0.0843, R_{sig} = 0.0363), N_o ($I > 2\sigma(I)$) = 3940; R = 0.0524, $wR2$ = 0.1324 (A,B = 0.10, 0), GOF = 1.006; $|\Delta\rho_{max}|$ = 0.31(5) e Å^{-3}.

Crystal/Refinement Details for 3. $C_{13}H_{10}N_2O_6$, M = 290.23, red needle 0.12 × 0.06 × 0.05 mm, $F(000)$ = 600 e, triclinic, $P\bar{1}$ (No. 2), Z = 4, T = 100(2) K, a = 9.547(7), b = 11.459(4), c = 12.227(6) Å, α = 75.44(3), β = 89.25(5), γ = 71.88(4)°, V = 1227.5(11) Å^3; D_c = 1.571 g cm^{-3}; $\sin\theta/\lambda_{max}$ = 0.5878; N(unique) = 4129 (merged from 15247, R_{int} = 0.1051, R_{sig} = 0.1849), N_o ($I > 2\sigma(I)$) = 1499; R = 0.0553, $wR2$ = 0.0984 (A,B = 0.02, 0), GOF = 1.002; $|\Delta\rho_{max}|$ = 0.24(6) e Å^{-3}.

Acknowledgment. We thank the Australian Research Council for support of this work and the University of Western Australia for a University Postgraduate Award to A.M.

Supporting Information Available: Crystallographic information files (CIF) for all three structures. This material is available free of charge via the Internet at http://pubs.acs.org.

References

(1) ten Brinke, G.; Ikkala, O.; Ruokolainen, J.; Saariaho, M.; Serimaa, R.; Thomas, E. L.; Torkkeli, M. *Macromolecules* **1999**, *32*, 1152.
(2) Chomczynski, P.; Sacci, N. *Anal. Biochem.* **1987**, *162*, 156.
(3) Chen, Y. X.; Fu, P. F.; Marks, T. J. *Organomet.* **1997**, *16*, 5958.
(4) Baekeland, L. H. *J. Ind. Eng. Chem.* (*U.S.A.*) **1909**, *1*, 149.
(5) Gutsche, C. D. *Calixarenes*, 2nd ed.; Royal Society of Chemistry Publishing: Cambridge, UK, 2008.
(6) Gutsche, C. D; Stewart, D. R. *J. Am. Chem. Soc.* **1999**, *121*, 4136.
(7) (a) Asfari, Z.; Souley, B.; Vicens, J. *Pol. J. Chem.* **1992**, *66*, 959. (b) J. L. Atwood, J. L.; Barbour, L. J.; Nichols, P. J.; Raston, C. L.; Sandoval, C. A. *Chem.—Eur. J.* **1999**, *5*, 990.
(8) Makha, M.; Raston, C. L. *Chem Commun.* **2001**, 2470.
(9) Barbour, L. J.; Makha, M.; Raston, C. L.; Sobolev, A. N.; Turner, P. *CrystEngComm* **2006**, *8*, 306.
(10) Prescott, L. F. *Paracetamol* (*Acetaminophen*)*: A Critical Bibliographic Review*, 1st ed; CRC Press: Boca Raton, FL, 1996.
(11) Bohmer, V.; Frings, M.; Paulus, E. F.; Schmidt, C.; Shivanyuk, A.; Vogt, W. *J. Chem. Soc., Perkin Trans. 2* **1998**, 2777.
(12) Gunduz, N.; Kilic, Z. *Tetrahedron* **1986**, *42*, 137.
(13) Jayatilaka, D.; McKinnon, J. J.; Spackman, M. A. *Chem Commun.* **2007**, 3814.
(14) McKinnon, J. J.; Mitchell, A. S.; Spackman, M. A. *Acta Crystallogr., Sect. B* **2004**, *60*, 627.
(15) Martin, A. D.; Raston, C. L.; Sobolev, A. N. *CrystEngComm.* **2010**, *15*, 2666.
(16) Makha, M.; McKinnon, J. J.; Sobolev, A. N.; Spackman, M. A.; Raston, C. L. *Chem.—Eur. J.* **2007**, *13*, 3907.
(17) Jayatilaka, D.; Spackman, M. A. *CrystEngComm* **2009**, *11*, 19.
(18) Marsh, R. E.; Schomaker, V.; Herbstein, F. H. *Acta Crystallogr., Sect. B* **1998**, *54*, 921.
(19) Sheldrick, G. M. *Acta Crystallogr., Sect. A* **2008**, *64*, 112.
(20) Barbour, L. J. *J. Supramol. Chem.* **2001**, *1*, 189.
(21) Grimwood, D. J.; Jayatilaka, D.; McKinnon, J. J.; Spackmann, M. A.; Wolff, S. K. *CrystalExplorer 2.1*; The University of Western Australia, 2008.